Chapter 9

Noise and Frequency Control

So far we only considered the deterministic steady state pulse formation in ultrashort pulse laser systems due to the most important pulse shaping mechanisms prevailing in todays femtosecond lasers. Due to the recent interest in using modelocked lasers for frequency metrology and high-resolution laser spectroscopy as well as phase sensitive nonlinear optics the noise and tuning properties of mode combs emitted by modelocked lasers is of much current interest. Soliton-perturbation theory is well suited to successfully predict the noise behavior of many solid-state and fiber laser systems [1] as well as changes in group- and phase velocity in modelocked lasers due to intracavity nonlinear effects [5]. We start off by reconsidering the derivation of the master equation for describing the pulse shaping effects in a mode-locked laser. We assume that in steady-state the laser generates at some position z (for example at the point of the output coupler) inside the laser a sequence of pulses with the envelope $a(T = mT_r, t)$. These envelopes are the solutions of the corresponding master equation, where the dynamics per roundtrip is described on a slow time scale $T = mT_R$. Then the pulse train emitted from the laser including the carrier is

$$A(T,t) = \sum_{m=-\infty}^{+\infty} a(T = mT_r, t) e^{j\left[\omega_c\left((t-mT_R+\left(\frac{1}{v_g}-\frac{1}{v_p}\right)2mL\right)\right]}. \qquad (9.1)$$

with repetition rate $f_R = 1/T_R$ and center frequency ω_c. Both are in general subject to slow drifts due to mirror vibrations, changes in intracavity pulse energy that might be further converted into phase and group velocity changes. Note, the center frequency and repetition rate are only defined for times long

compared to the roundtrip time in the laser. Usually, they only change on a time scale three orders of magnitude longer than the expectation value of the repetition rate.

9.1 The Mode Comb

Lets suppose the pulse envelope, repetition rate, and center frequency do not change any more. Then the corresponding time domain signal is sketched in Figure 9.1.

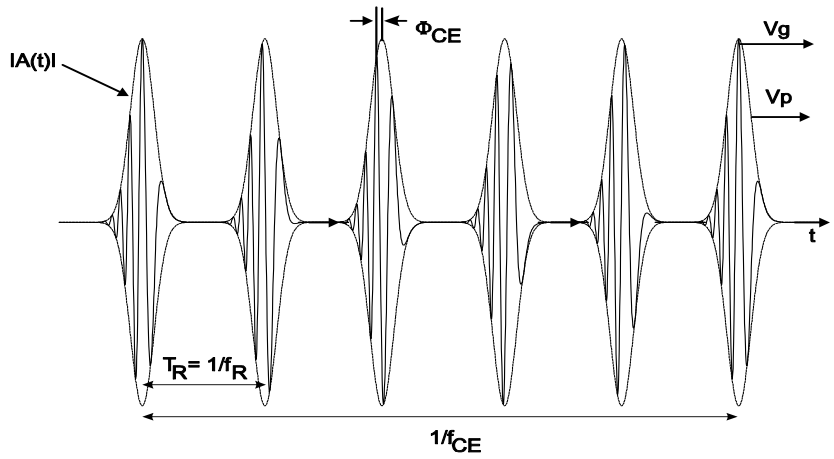

Figure 9.1: Pulse train emitted from a noise free mode-locked laser. The pulses can have chirp. The intensity envelope repeats itself with repetition rate f_R. The electric field is only periodic with the rate f_{CE} if it is related to the repetion rate by a rational number.

The pulse $a(T = mT_r, t)$ is the steady state solution of the master equation describing the laser system, as studied in chapter 6. Let's assume that the steady state solution is a purturbed soliton according to equation (6.64).

$$a(t,T) = \left(A_0 \,\mathrm{sech}(\frac{t-t_0}{\tau}) + a_c(T,t) \right) e^{-j\phi_0 \frac{T}{T_R}} \tag{9.2}$$

with the soliton phase shift

$$\phi_0 = \frac{1}{2}\delta A_0^2 = \frac{|D|}{\tau^2} \tag{9.3}$$

Thus, there is a carrier envelope phase shift $\Delta\phi_{CE}$ from pulse to pulse given by

$$\begin{aligned}\Delta\phi_{CE} &= \left(\frac{1}{v_g}-\frac{1}{v_p}\right)\Big|_{\omega_c} 2L-\phi_0+\mathrm{mod}(2\pi) \\ &= \omega_c T_R\left(1-\frac{v_g}{v_p}\right)-\phi_0+\mathrm{mod}(2\pi)\end{aligned} \tag{9.4}$$

The Fourier transform of the unperturbed pulse train is

$$\begin{aligned}\hat{A}(\omega) &= \hat{a}(\omega-\omega_c)\sum_{m=-\infty}^{+\infty} e^{j(\Delta\phi_{CE}-(\omega-\omega_c)T_R)m} \\ &= \hat{a}(\omega-\omega_c)\sum_{n=-\infty}^{+\infty} e^{jmT_R\left(\frac{\Delta\phi_{CE}}{T_R}-\omega\right)} \\ &= \hat{a}(\omega-\omega_c)\sum_{n=-\infty}^{+\infty} T_R\delta\left(\omega-\left(\frac{\Delta\phi_{CE}}{T_R}+n\omega_R\right)\right)\end{aligned} \tag{9.5}$$

which is shown in Figure 9.2. Each comb line is shifted by the carrier-envelope offset frequency $f_{CE}=\frac{\Delta\phi_{CE}}{2\pi T_R}$ from the origin

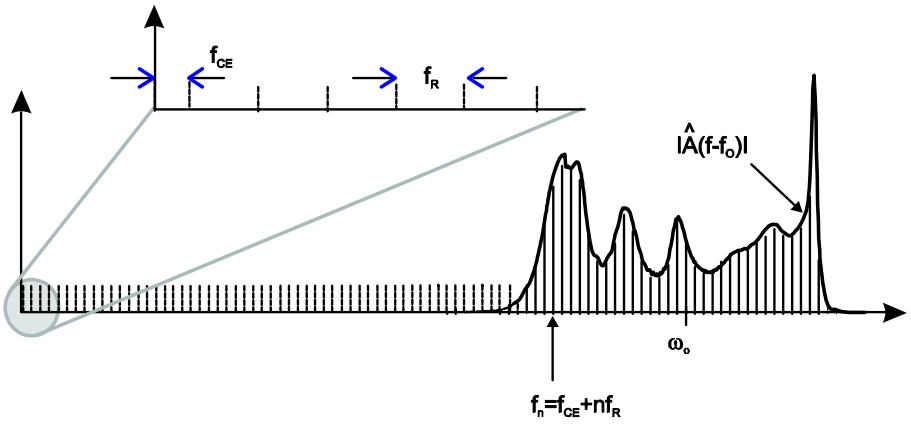

Figure 9.2: Opitcal mode comb of a mode-locked laser output.

To obtain self-consistent equations for the repetition rate, center frequency and the other pulse parameters we employ soliton-perturbation theory. This is justified for the case, where the steady state pulse is close to a

soliton, i.e. for the fast saturable absorber case, this is the chirp free solution, occuring when the ratio of gain filtering to dispersion is equal to the ratio of SAM action to self-phase modulation, see Eq. (6.61). Then the pulse solution in the $m-$th roundtrip is a solution of the nonlinear Schrödinger Equation stabilized by the irreversible dynamics and subject to additional perturbations

$$\begin{aligned} T_R \frac{\partial}{\partial T} A &= jD \frac{\partial^2}{\partial t^2} A - j\delta |A|^2 A \\ &\quad + (g-l)A + D_f \frac{\partial^2}{\partial t^2} A + \gamma |A|^2 A + L_{\text{pert}} \end{aligned} \tag{9.6}$$

Due to the irreversible processes and the perturbations the solution to (9.6) is a soliton like pulse with perturbations in amplitude, phase, frequency and timing plus some continuum

$$\begin{aligned} A(t,T) &= [(A_o + \Delta A_o)\,\text{sech}[(t-\Delta t)/\tau] + a_c(T,t)] \\ &\quad e^{-j\phi_o T/T_R} e^{j\Delta p(T)t} e^{-j\theta_0} \end{aligned} \tag{9.7}$$

with pulse energy $w_0 = 2A_o^2\tau$.

The perturbations cause fluctuations in amplitude, phase, center frequency and timing of the soliton and generate background radiation, i.e. continuum

$$\begin{aligned} \Delta A(T,t) &= \Delta w(T) f_w(t) + \Delta\theta(T) f_\theta(t) + \Delta p(T) f_p(t) \\ &\quad + \Delta t(T) f_t(t) + a_c(T,t). \end{aligned} \tag{9.8}$$

where, we rewrote the amplitude perturbation as an energy perturbation. The dynamics of the pulse parameters due to the perturbed Nonlinear Schrödinger Equation (9.6) can be projected out from the perturbation using the adjoint basis and the orthogonality relation, see Chapter 3.5. Note, that the f_i correspond to the first component of the vector in Eqs.(3.22) - (3.25). The dynamics of the pulse parameters due to the perturbed Nonlinear Schrödinger Equation (9.6) can be projected out from the perturbation using the adjoint basis $\bar{f}_i^*$ corresponding to the first component of the vector in Eqs.(3.44) - (3.47) and the new orthogonality relation

$$\text{Re}\left\{ \int_{-\infty}^{+\infty} \bar{f}_i^*(t) f_j(t) dt \right\} = \delta_{i,j}. \tag{9.9}$$

We obtain

$$\frac{\partial}{\partial T}\Delta w = -\frac{1}{\tau_w}\Delta w + \frac{1}{T_R}\mathrm{Re}\left\{\int_{-\infty}^{+\infty} \bar{f}_w^*(t) L_{\mathrm{pert}}(T,t)dt\right\} \quad (9.10)$$

$$\frac{\partial}{\partial T}\Delta\theta(T) = \frac{2\phi_o}{T_R}\frac{\Delta w}{w_o} + \frac{1}{T_R}\mathrm{Re}\left\{\int_{-\infty}^{+\infty} \bar{f}_\theta^*(t) L_{\mathrm{pert}}(T,t)dt\right\} \quad (9.11)$$

$$\frac{\partial}{\partial T}\Delta p(T) = -\frac{1}{\tau_p}\Delta p + \frac{1}{T_R}\mathrm{Re}\left\{\int_{-\infty}^{+\infty} \bar{f}_p^*(t) L_{\mathrm{pert}}(T,t)dt\right\} \quad (9.12)$$

$$\frac{\partial}{\partial T}\Delta t = \frac{-2|D|}{T_R}\Delta\omega + \frac{1}{T_R}\mathrm{Re}\left\{\int_{-\infty}^{+\infty} \bar{f}_t^*(t) L_{\mathrm{pert}}(T,t)dt\right\} \quad (9.13)$$

Note, that the irreversible dynamics does couple back the generated continuum to the soliton parameters. Here, we assume that this coupling is small and neglect it in the following, see [1]. Due to gain saturation and the parabolic filter pulse energy and center frequency fluctuations are damped with normalized decay constants

$$\frac{1}{\tau_w} = (2g_d - 2\gamma A_o^2) \quad (9.14)$$

$$\frac{1}{\tau_p} = \frac{4}{3}\frac{g_s}{\Omega_g^2\tau^2}\frac{1}{T_R} \quad (9.15)$$

Here, g_s is the saturated gain and g_d is related to the differential gain by

$$g_s = \frac{g_o}{1 + \frac{w_o}{P_L T_R}} \quad (9.16)$$

$$g_d = \frac{dg_s}{dw_o}\cdot w_o \quad (9.17)$$

Note, in this model we assumed that the gain instantaneously follows the intracavity average power or pulse energy, which is not true in general. However, it is straight forward to include the relaxation of the gain by adding a dynamical gain model to the perturbation equations. For simplicity we shall neglect this here. Since the system is autonomous, there is no retiming and rephasing in the free running system.

9.2 Noise in Mode-locked Lasers

Within this framework the response of the laser to noise can be easily included. The spontaneous emission noise due to the amplifying medium with saturated gain g_s and excess noise factor Θ leads to additive white noise in the perturbed master equation (9.6) with $L_{\text{pert}} = \xi(t,T)$, where ξ is a white Gaussian noise source with autocorrelation function

$$\langle \xi(t',T')\xi(t,T)\rangle = T_R^2 P_n \delta(t-t')\delta(T-T') \tag{9.18}$$

where the spontaneous emission noise energy $P_n \cdot T_R$ with

$$P_n = \Theta \frac{2g_s}{T_R}\hbar\omega_c = \Theta\frac{\hbar\omega_c}{\tau_p} \tag{9.19}$$

is added to the pulse within each roundtrip in the laser. τ_p is the cavity decay time or photon lifetime in the cavity. Note, that the noise is approximated by white noise, i.e. uncorrelated noise on both time scales t, T. The noise between different round-trips is certainly uncorrelated. However, white noise on the fast time scale t, assumes a flat gain, which is an approximation. By projecting out the equations of motion for the pulse parameters in the presence of this noise according to (9.8)–(9.13), we obtain the additional noise sources which are driving the energy, center frequency, timing and phase fluctuations in the mode-locked laser

$$\frac{\partial}{\partial T}\Delta w = -\frac{1}{\tau_w}\Delta w + S_w(T), \tag{9.20}$$

$$\frac{\partial}{\partial T}\Delta\theta(T) = \frac{2\phi_o}{T_R}\frac{\Delta w}{w_o} + S_\theta(T), \tag{9.21}$$

$$\frac{\partial}{\partial T}\Delta p(T) = -\frac{1}{\tau_p}\Delta p + S_p(T), \tag{9.22}$$

$$\frac{\partial}{\partial T}\Delta t = \frac{-2|D|}{T_R}\Delta p + S_t(T), \tag{9.23}$$

with

$$S_w(T) = \frac{1}{T_R}\mathrm{Re}\left\{\int_{-\infty}^{+\infty} \bar{f}_w^*(t)\xi(T,t)dt\right\}, \tag{9.24}$$

$$S_\theta(T) = \frac{1}{T_R}\mathrm{Re}\left\{\int_{-\infty}^{+\infty} \bar{f}_\theta^*(t)\xi(T,t)dt\right\}, \tag{9.25}$$

$$S_p(T) = \frac{1}{T_R}\mathrm{Re}\left\{\int_{-\infty}^{+\infty} \bar{f}_p^*(t)\xi(T,t)dt\right\}, \tag{9.26}$$

$$S_t(T) = \frac{1}{T_R}\mathrm{Re}\left\{\int_{-\infty}^{+\infty} \bar{f}_t^*(t)\xi(T,t)dt\right\}. \tag{9.27}$$

The new reduced noise sources obey the correlation functions

$$\langle S_w(T')S_w(T)\rangle = \frac{P_n}{4w_0}\delta(T-T'), \tag{9.28}$$

$$\langle S_\theta(T')S_\theta(T)\rangle = \frac{4}{3}\left(1+\frac{\pi^2}{12}\right)\frac{P_n}{w_o}\delta(T-T'), \tag{9.29}$$

$$\langle S_p(T')S_p(T)\rangle = \frac{4}{3}\frac{P_n}{w_o}\delta(T-T'), \tag{9.30}$$

$$\langle S_t(T')S_t(T)\rangle = \frac{\pi^2}{3}\frac{P_n}{w_o}\delta(T-T'), \tag{9.31}$$

$$\langle S_i(T')S_j(T)\rangle = 0 \text{ for } i \neq j. \tag{9.32}$$

The power spectra of amplitude, phase, frequency and timing fluctuations are defined via the Fourier transforms of the autocorrelation functions

$$|\Delta\hat{w}(\Omega)|^2 = \int_{-\infty}^{+\infty}\langle\Delta\hat{w}(T+\tau)\Delta\hat{w}(T)\rangle e^{-j\Omega\tau}d\tau, \text{ etc.} \tag{9.33}$$

After a short calculation, the power spectra due to amplifier noise are

$$\left|\frac{\Delta\hat{w}(\Omega)}{w_o}\right|^2 = \frac{4}{1/\tau_w^2+\Omega^2}\frac{P_n}{w_o}, \tag{9.34}$$

$$|\Delta\hat{\theta}(\Omega)|^2 = \frac{1}{\Omega^2}\left[\frac{4}{3}\left(1+\frac{\pi^2}{12}\right)\frac{P_n}{w_o} + \frac{16}{(1/\tau_p^2+\Omega^2)}\frac{\phi_o^2}{T_R^2}\frac{P_n}{w_o}\right], \tag{9.35}$$

$$|\Delta\hat{p}(\Omega)\tau|^2 = \frac{1}{1/\tau_p^2+\Omega^2}\frac{4}{3}\frac{P_n}{w_o}, \tag{9.36}$$

$$\left|\frac{\Delta\hat{t}(\Omega)}{\tau}\right|^2 = \frac{1}{\Omega^2}\left[\frac{\pi^2}{3}\frac{P_n}{w_o} + \frac{1}{(1/\tau_\omega^2+\Omega^2)}\frac{4}{3}\frac{4|D|^2}{T_R^2\tau^4}\frac{P_n}{w_o}\right]. \tag{9.37}$$

These equations indicate, that energy and center frequency fluctuations become stationary with mean square fluctuations

$$\left\langle \left(\frac{\Delta w}{w_o} \right)^2 \right\rangle = 2 \frac{P_n \tau_w}{w_o} \tag{9.38}$$

$$\langle (\Delta\omega\tau)^2 \rangle = \frac{2}{3} \frac{P_n \tau_p^2}{w_o} \tag{9.39}$$

whereas the phase and timing undergo a random walk with variances

$$\begin{aligned} \sigma_\theta(T) &= \langle (\Delta\theta(T) - \Delta\theta(0))^2 \rangle = \frac{4}{3} \left(1 + \frac{\pi^2}{12} \right) \frac{P_n}{w_o} |T| \\ &+16 \frac{\phi_o^2}{T_R^2} \frac{P_n}{w_o} \tau_p^3 \left(\exp\left[-\frac{|T|}{\tau_p} \right] - 1 + \frac{|T|}{\tau_w} \right) \end{aligned} \tag{9.40}$$

$$\begin{aligned} \sigma_t(T) &= \left\langle \left(\frac{\Delta t(T) - \Delta t(0)}{\tau} \right)^2 \right\rangle = \frac{\pi^2}{3} \frac{P_n}{w_o} |T| \\ &+\frac{4}{3} \frac{4|D|^2}{T_R^2 \tau^4} \frac{P_n}{w_o} \tau_\omega^3 \left(\exp\left[-\frac{|T|}{\tau_p} \right] - 1 + \frac{|T|}{\tau_p} \right) \end{aligned} \tag{9.41}$$

The phase noise causes the fundamental finite width of every line of the mode-locked comb in the optical domain. The timing jitter leads to a finite linewidth of the detected microwave signal, which is equivalent to the lasers fundamental fluctuations in repetition rate. In the strict sense, phase and timing in a free running mode-locked laser (or autonomous oscillator) are not anymore stationary processes. Nevertheless, since we know these are Gaussian distributed variables, we can compute the amplitude spectra of phasors undergoing phase diffusion processes rather easily. The phase difference $\varphi = \Delta\theta(T) - \Delta\theta(0)$ is a Gaussian distributed variable with variance σ and propability distribution

$$p(\varphi) = \frac{1}{\sqrt{2\pi\sigma}} e^{-\frac{\varphi^2}{2\sigma}}, \text{ with } \sigma = \left\langle \varphi^2 \right\rangle . \tag{9.42}$$

Therefore, the expectation value of a phasor with phase φ is

$$\begin{aligned} \left\langle e^{j\varphi} \right\rangle &= \frac{1}{\sqrt{2\pi\sigma}} \int_{-\infty}^{+\infty} e^{-\frac{\varphi^2}{2\sigma}} e^{j\varphi} d\varphi \\ &= e^{-\frac{1}{2}\sigma}. \end{aligned} \tag{9.43}$$

9.2.1 The Optical Spectrum

$$a(t,T) = \left(A_0 \,\mathrm{sech}(\frac{t-t_0}{\tau}) + a_c(T,t) \right) e^{-j\phi_0 \frac{T}{T_R}} \tag{9.44}$$

In the presence of noise the laser output changes from eq.(9.1) to a random process. Neglecting the background continuum we obtain:

$$A(t,T = mT_R) = \sum_{m=-\infty}^{+\infty} (A_0 + \Delta A(mT_R)) \,\mathrm{sec\,h}\left(\frac{t - mT_R - \Delta t(mT_R)}{\tau} \right) \tag{9.45}$$
$$e^{j\Delta\phi_{CE}\cdot m} e^{j(\omega_c + \Delta p(mT_R))t} e^{-j\Delta\theta(mT_R)}$$

For simplicity, we will neglect in the following amplitude and carrier frequency fluctuations in Eq.(9.45), because they are bounded and become only important at large offsets from the comb. However, we keep them in the expressions for the phase and timing jitter Eqs.(9.34) and (9.36). We assume a stationary process, so that the optical power spectrum can be computed from

$$S(\omega) = \lim_{T=2NT_R \to \infty} \frac{1}{T} \langle \hat{A}_T^*(\omega) \hat{A}_T(\omega) \rangle \tag{9.46}$$

with the spectra related to a finite time interval

$$\hat{A}_T(\omega) = \int_{-T}^{T} A(t) e^{-j\omega t} dt = \hat{a}_0(\omega - \omega_c) \sum_{m=-N}^{N} e^{jmT_R\left(\frac{\Delta\phi_{CE}}{T_R} - \omega\right)} \tag{9.47}$$
$$e^{-j[(\omega-\omega_c)\Delta t(mT_R) + \Delta\theta(mT_R)]}$$

where $\hat{a}_0(\omega)$ is the Fourier transform of the pulse shape. In this case

$$\hat{a}_0(\omega) = \int_{-\infty}^{\infty} A_0 \,\mathrm{sec\,h}\left(\frac{t}{\tau}\right) e^{-j\omega t} dt = A_0 \pi\tau \,\mathrm{sec\,h}\left(\frac{\pi}{2}\omega\tau\right) \tag{9.48}$$

With (9.46) the optical spectrum of the laser is given by

$$S(\omega) = \lim_{N\to\infty} |\hat{a}_0(\omega - \omega_c)|^2 \frac{1}{2NT_R} \sum_{m'=-N}^{N} \sum_{m=-N}^{M} e^{jT_R\left(\frac{\phi_{CE}}{T_R} - \omega\right)(m-m')} \tag{9.49}$$
$$\left\langle e^{+j[2\pi(f-f_c)(\Delta t(mT_R) - \Delta t(m'T_R)) - (\theta(mT_R) - \theta(m'T_R))]} \right\rangle$$

Note, that the difference between the phases and the timing only depends on the difference $k = m - m'$. In the current model phase and timing fluctuations are uncorrelated. Therefore, for $N \to \infty$ we obtain

$$\begin{aligned} S(\omega) &= |\hat{a}_0(\omega-\omega_c)|^2 \tfrac{1}{T_R} \textstyle\sum_{k'=-\infty}^{\infty} e^{jT_R\left(\frac{\Delta\phi_{CE}}{T_R}-\omega\right)k} \\ &\quad \left\langle e^{+j[2\pi(\omega-\omega_0)(\Delta t((m+k)T_R)-\Delta t(mT_R))]}\right\rangle \left\langle e^{-j(\theta((m+k)T_R)-\theta(mT_R))}\right\rangle . \end{aligned} \tag{9.50}$$

The expectation values are exactly of the type calculated in (9.43), which leads to

$$\begin{aligned} S(\omega) &= \frac{|\hat{a}_0(\omega-\omega_c)|^2}{T_R} \sum_{k'=-\infty}^{\infty} e^{jT_R\left(\frac{\phi_{CE}}{T_R}-\omega\right)k} e^{-\frac{1}{2}\sigma_\theta(kT_R)} \\ &\quad e^{-\frac{1}{2}\left[((\omega-\omega_c)\tau)^2\sigma_t(kT_R)\right]} \end{aligned} \tag{9.51}$$

Most often we are interested in the noise very close to the lines at frequency offsets much smaller than the inverse energy and frequency relaxation times τ_w and τ_p. This is determined by the long term behavior of the variances, which grow linearly in $|T|$

$$\sigma_\theta(T) = \frac{4}{3}\left(1+\frac{\pi^2}{12}+16\frac{\tau_w^2}{T_R^2}\phi_o^2\right)\frac{P_n}{w_o}|T| = 2\Delta\omega_\phi|T|, \tag{9.52}$$

$$\sigma_t(T) = \frac{1}{3}\left(\pi^2+\frac{\tau_p^2}{T_R^2}\left(\frac{D}{\tau^2}\right)^2\right)\frac{P_n}{w_o}|T| = 4\Delta\omega_t|T|. \tag{9.53}$$

with the rates

$$\Delta\omega_\phi = \frac{2}{3}\left(1+\frac{\pi^2}{12}+16\frac{\tau_w^2}{T_R^2}\phi_o^2\right)\frac{P_n}{w_o}, \tag{9.54}$$

$$\Delta\omega_t = \frac{1}{6}\left(\pi^2+\frac{\tau_p^2}{T_R^2}\left(\frac{D}{\tau^2}\right)^2\right)\frac{P_n}{w_o}. \tag{9.55}$$

From the Poisson formula

$$\sum_{k=-\infty}^{+\infty} h[k]e^{-jkx} = \sum_{n=-\infty}^{+\infty} G(x+2n\pi) \tag{9.56}$$

where

$$G(x) = \int_{-\infty}^{+\infty} h[k] e^{-jkx} dk, \tag{9.57}$$

and Eqs.(9.51) to (9.55) we finally arrive at the optical line spectrum of the mode-locked laser

$$S(\omega) = \frac{|\hat{a}_0(\omega - \omega_c)|^2}{T_R^2} \sum_{n=-\infty}^{+\infty} \frac{2\Delta\omega_n}{(\omega - \omega_n)^2 + \Delta\omega_n^2} \tag{9.58}$$

which are Lorentzian lines at the mode comb positions

$$\omega_n = \omega_c + n\omega_R - \frac{\Delta\phi_{CE}}{T_R}, \tag{9.59}$$

$$= \frac{\Delta\phi_{CE}}{T_R} + n'_R\omega, \tag{9.60}$$

with a half width at half maximum of

$$\Delta\omega_n = \Delta\omega_\phi + [\tau(\omega_n - \omega_c)]^2 \Delta\omega_t. \tag{9.61}$$

Estimating the number of modes M included in the comb by

$$M = \frac{T_R}{\tau}, \tag{9.62}$$

we see that the contribution of the timing fluctuations to the linewidth of the comb lines in the center of the comb is negligible. Thus the linewidth of the comb in the center is given by 9.54

$$\Delta\omega_\phi = \frac{2}{3}\left(1 + \frac{\pi^2}{12} + 16\frac{\tau_w^2}{T_R^2}\phi_o^2\right)\frac{\Theta 2 g_s}{N_0 T_R} \tag{9.63}$$

$$= \frac{2}{3}\left(1 + \frac{\pi^2}{12} + 16\frac{\tau_w^2}{T_R^2}\phi_o^2\right)\frac{\Theta}{N_0 \tau_p} \tag{9.64}$$

where $N_0 = \frac{w_o}{\hbar\omega_c}$ is the number of photons in the cavity and $\tau_p = T_R/(2l)$ is the photon lifetime in the cavity. Note that this result for the mode-locked laser is closely related to the Schawlow-Towns linewidth of a continuous wave laser which is $\Delta f_\phi = \frac{\Theta}{2\pi N_0 \tau_p}$. For a solid-state laser at around $1\mu m$ wavelength with a typical intracavity pulse energy of 50 nJ corresponding to $N_0 = 2.5 \cdot 10^{11}$ photons and 100 MHz repetition rate with a 10% output coupler and an

excess noise figure of $\Theta = 2$, we obtain $\Delta f_{\phi}\tilde{} \frac{\Theta}{3\pi N_0 \tau_p} = 8\mu Hz$ without the amplitude to phase conversion term depending on the nonlinear phase shift ϕ_o. These intrinsic linewidths are due to fluctuations happening on a time scale faster than the round-trip time and, therefore, can not be compensated by external servo control mechanisms. For sub-10 fs lasers, the spectra fill up the full gain bandwidth and the KLM is rather strong, so that the amplitude and center frequency relaxation times are on the order of 10-100 cavity roundtrips. In very short pulse Ti:sapphire lasers nonlinear phase shifts are on the order of 1 rad per roundtrip. Then most of the fluctuations are due to amplitude fluctuations converted into phase jitter. This contributions can increase the linewidth by a factor of 100-10000, which may bring the linewidth to the mHz and Hz level.

9.2.2 The Microwave Spectrum

Not only the optical spectrum is of interest als the spectrum of the photo detected output of the laser is of intrest. Simple photo detection can convert the low jitter optical pulse stream into a comb of extremely low phase noise microwave signals. The photo detector current is proportional to the output power of the laser. From Eq.(9.45) we find

$$\begin{aligned} I(t) &= \eta \frac{e}{\hbar\omega_c} |A(T,t)|^2 = \eta \frac{e}{\hbar\omega_c \tau} \times \\ &\sum_{m=-\infty}^{+\infty} (w_0 + \Delta w(mT_R)) \frac{1}{2} \sec \mathrm{h}^2 \left(\frac{t - mT_R - \Delta t(mT_R)}{\tau} \right), \end{aligned} \tag{9.65}$$

where η is the quantum efficiency. For simplicity we neglect again the amplitude noise and consider only the consequences due to the timing jitter. Then we obtain for the Fourier Transform of the photo current

$$\hat{I}_T(\omega) = \eta \frac{e w_0}{\hbar\omega_0 \tau} |a_0|^2 (\omega) \sum_{m=-N}^{+N} e^{-j\omega(mT_R + \Delta t(mT_R))}, \tag{9.66}$$

$$\begin{aligned} |a_0|^2 (\omega) &= \int_{-\infty}^{\infty} \frac{1}{2} \sec \mathrm{h}^2 (x) \; e^{-j\omega\tau x} dx & (9.67) \\ &= \frac{\pi\omega\tau}{\sinh(\frac{\pi}{2}\omega\tau)}, & (9.68) \end{aligned}$$

and its power spectrum according to Eq.(9.46)

$$\begin{aligned} S_I(\omega) &= \frac{(\eta e N_0)^2}{T_R} \left||a_0|^2(\omega)\right|^2 \sum_{k=-\infty}^{+\infty} e^{-j\omega k T_R} \left\langle e^{-j\omega(\Delta t(kT_R)-\Delta t(0))} \right\rangle, \\ &= \frac{(\eta e N_0)^2}{T_R} \left||a_0|^2(\omega)\right|^2 \sum_{k=-\infty}^{+\infty} e^{-j\omega k T_R} e^{-\frac{1}{2}\left[(\omega\tau)^2 \sigma_t(kT_R)\right]} \end{aligned} \tag{9.69}$$

Using the Poisson formula again results in

$$\begin{aligned} S_I(\omega) &= \frac{(\eta e N_0)^2}{T_R} \left||a_0|^2(\omega)\right|^2 \sum_{k=-\infty}^{+\infty} e^{-j\omega k T_R} e^{-j\omega(\Delta t(kT_R)-\Delta t(0))}, \\ &= \frac{(\eta e N_0)^2}{T_R^2} \left||a_0|^2(\omega)\right|^2 \sum_{n=-\infty}^{+\infty} \frac{2\Delta\omega_{I,n}}{(\omega - n\omega_R)^2 + \Delta\omega_{I,n}^2} \end{aligned} \tag{9.70}$$

with the linewidth $\Delta\omega_{I,n}$ of the n-th harmonic

$$\begin{aligned} \Delta\omega_{I,n} &= \left(2\pi n \frac{\tau}{T_R}\right)^2 \Delta\omega_t \\ &= \left(\frac{2\pi n}{M}\right)^2 \Delta\omega_t. \end{aligned} \tag{9.71}$$

The fundamental line ($n = 1$) of the microwave spectrum has a width which is M^2-times smaller than the optical linewidth. For a 10-fs laser with 100 MHz repetition rate, the number of modes M is about a million.

9.2.3 Example: Yb-fiber laser:

Figure 9.3 shows the schematic of a streched pulse modelocked laser operating close to zero dispersion. Therefore, the contribution of the Gordon-Haus jitter should be minimized. Infact, it has been shown and discussed that these types of lasers reach minimum jitter levels [2][3][4].

The timing jitter of the streched pulse laser shown in Figure is computed in table 9.1.

The theoretical results above are derived with soliton perturbation theory. The stretched pulse modelocked laser in Figure 9.3 is actually far from being a soliton laser, see [3][4]. The pulse is breathing considerably during

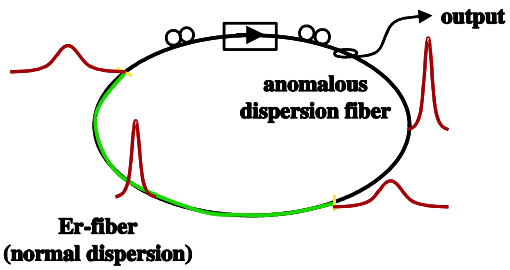

Figure 9.3: Schematic of a streched pulse modelocked laser.

Gain Half-Width Half Maximum	$\Omega_g = 2\pi \cdot \frac{0.3\mu\text{m/fs}}{(1.\mu\text{m})^2} 0.02\mu\text{m} = 38\text{THz}$
Saturated gain	$g_s = 1.2$
Pulse width	$\tau_{FWHM} = 50\text{fs}$, $\tau = \tau_{FWHM}/1.76 = 30fs$
Pulse repetition time	$T_R = 12ns$
Decay time for center freq. fluctuations	$\frac{1}{\tau_p} = \frac{4}{3}\frac{g_s}{\Omega_g^2 \tau^2 T_R} = \frac{4}{3}\frac{1}{T_R}$
Intracavity power	$P = 100\text{mW}$
Intra cavity pulse energy / photon number	$w_o = 1.2\text{nJ}, \quad N_0 = 0.6 \cdot 10^{10}$
Noise power spectral density	$P_n = \Theta \frac{2g_s}{T_R} \hbar\omega_o$
Amplifier excess noise factor	$\Theta = 10$
ASE noise	$\frac{P_n}{w_o} = \Theta \frac{2g_s}{T_R N_0} = \frac{1}{3} Hz$
Dispersion	$5000 fs^2$
Frequency-to-timing conv.	$\frac{4}{\pi^2}\frac{4\lvert D\rvert^2}{\tau^4}\frac{\tau_p^2}{T_R^2} = \left(\frac{2}{\pi}\frac{3}{4}\frac{3\cdot 10000}{1000}\right)^2 = (3.7)^2$
Timing jitter density	$\left\lvert\frac{\Delta\hat{t}(\Omega)}{\tau}\right\rvert^2 = \frac{1}{\Omega^2}\frac{\pi^2}{3}\frac{P_n}{w_o}\left(1 + \frac{4}{\pi^2}\frac{4\lvert D\rvert^2}{\tau^4}\frac{1}{(T_R^2/\tau_p^2 + T_R^2\Omega^2)}\right)$
Timing jitter $[f_{\min}, f_{\max}]$ for $f_{\min} << 1/\tau_p$, $f_{\min} = 10kHz,\ D = 5000 fs^2$	$\Delta t = \tau\sqrt{\frac{1}{12\cdot f_{\min}}\frac{P_n}{w_o}\left(1 + \frac{4}{\pi^2}\frac{4\lvert D\rvert^2}{\tau^4}\frac{\tau_p^2}{T_R^2}\right)} = 0.2fs$

Table 9.1: Parameters for the streched pulse modelocked laser of Figure 9.3.

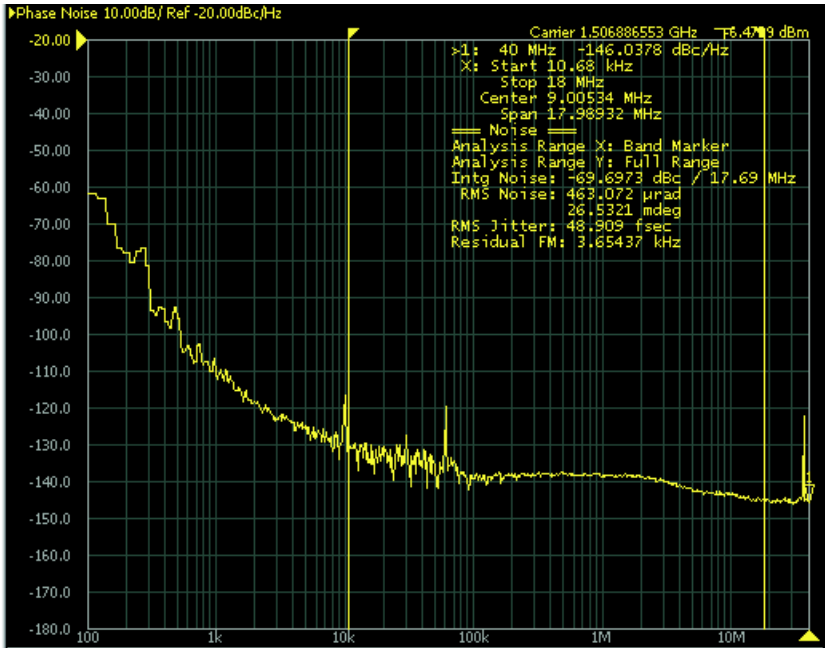

Figure 9.4: Timing jitter measurement of the output from the streched pulse modelocked laser measured with a HP 5504 signal analyzer.

passage through the cavity up to a factor of 10. Therefore, the theory should take that into account by assuming an average pulse width when the noise is added in the cavity. For more details see [3][4]. In reality, these quantum limited (ASE) and rather small optical and microwave linewidths are difficult to observe, because they are most often swamped by technical noise such as fluctuations in pump power, which may case gain fluctuations, or mirror vibrations, air-density fluctuations or thermal drifts, which directly cause changes in the lasers repetition rate. Figure 9.4 shows the single-sideband phase noise spectrum L(f) of the N=32nd harmonic of the fundamental repetition rate, i.e 1.3 GHz, in the photo current spectrum 9.70. The phase of the N=32nd harmonic of the photocurrent 9.65 is directly related to the timing jitter by

$$\Delta\varphi(T) = 2\pi N f_R \Delta t(T) \tag{9.72}$$

The single-sideband phase noise is the power spectral density of these phase fluctuations defined in the same way as the power spectral density of the

photocurrent itself, i.e.

$$L(f) = 2\pi S_{\Delta\varphi}(\omega) \tag{9.73}$$

The phase fluctuations in a certain frequency intervall can then be easily evaluated by

$$\Delta\varphi^2 = 2\int_{f\,\mathrm{min}}^{f\,\mathrm{max}} L(f)df. \tag{9.74}$$

And the timing jitter is then

$$\Delta t = \frac{1}{2\pi N f_R}\sqrt{2\int_{f\,\mathrm{min}}^{f\,\mathrm{max}} L(f)df}. \tag{9.75}$$

For the measurements shown in Figure 9.4 we obtain for the integrated timing jitter from 10kHz to 20 MHz of 50 fs. This is about 200 times larger than the limits derived in table 9.1. This discrepancy comes from several effects, most notable amplitude to phase conversion in the photodetector during photodetection, an effect not yet well understood as well as other noise sources we might not have modelled, such as noise from the pump laser. However, these noise sources can be eliminated in principle by careful design and feedback loops. Therefore, it is important to understand the dependence of the group and phase velocity on the intracavity power or pulse energy at least within the current basic model. Additional linear and nonlinear effects due to higher order linear dispersion or nonlinearities may cause additional changes in group and phase velocity, which might also create unusual dependencies of group and phase velocity on intracavity pulse energy. Here we discuss as an example the impact of the instantaneous Kerr effect on group and phase velocity of a soliton like pulse.

9.3 Group- and Phase Velocity of Solitons

The Kerr-effect leads to a change of phase velocity of the pulse, resulting in the self-phase shift of the soliton, ϕ_o, per round-trip. A change in group velocity does not appear explicitly in the solution of the NLSE. Self-steepening which becomes important for ultrashort pulses leads to an additional term in the NLSE and therefore to an additional term in the master equation (9.6)

$$L_{\mathrm{pert}} = -\frac{\delta}{\omega_c}\frac{\partial}{\partial t}(|a(T,t)|^2 a(T,t)). \tag{9.76}$$

The impact of this term is expected to be small of the order of $1/(\omega_o\tau)$ and therefore only important for few-cycle pulses. However, it turns out that this term alters the phase and group velocity of the soliton like pulse as much as the nonlinear phase shift itself. We take his term into account in form of a perturbation. This perturbation term is odd and real and therefore only leads to a timing shift, when substituted into Eq.(9.6).

$$T_R \frac{\partial \Delta t(T)}{\partial T}\bigg|_{sst} = -\frac{\delta}{\omega_c} A_0^3 \,\mathrm{Re}\left\{\int_{-\infty}^{+\infty} \bar{f}_t^*(t) \frac{\partial}{\partial t}\left(\sec h^3\left(\frac{t}{\tau}\right)\right) dt\right\} \quad (9.77)$$

$$= \frac{\delta}{\omega_c} A_0^2 = \frac{2\phi_0}{\omega_c}. \quad (9.78)$$

This timing shift or group delay per round-trip, together with the nonlinear phase shift leads to a phase change between carrier and envelope per roundtrip given by

$$\Delta\phi_{CE} = -\phi_0 + \omega_o\, T_R \frac{\partial}{\partial T}\Delta t(T)\bigg|_{selfsteep} = -\frac{1}{2}\delta A_0^2 + \delta A_0^2 = \frac{1}{2}\delta A_0^2. \quad (9.79)$$

The compound effect of this phase delay per round-trip in the carrier versus envelope leads to a carrier-envelope frequency

$$f_{CE} = \frac{\Delta\phi_{CE}}{2\pi} f_R = \frac{\phi_0}{2\pi} f_R. \quad (9.80)$$

The group delay also changes the optical cavity length of the laser and therefore alters the repetition rate according to

$$\Delta f_R = -f_R^2 \Delta t(T)\big|_{selfsteep} = -2\phi_0 \frac{f_R}{\omega_o} f_R = -\frac{2}{m_0} f_{CE}, \quad (9.81)$$

where m_0 is the mode number of the carrier wave. Eqs.(9.80) and (9.81) together determine the shift of the m-th line of the optical comb $f_m = f_{CE} + mf_R$ due to an intracavity pulse energy modulation and a change in cavity length by

$$\Delta f_m = \Delta f_{CE} + m\Delta f_R = f_{CE}\left(1 - \frac{2m}{m_0}\right)\frac{\Delta w}{w_0} - m f_R \frac{\Delta L}{L_0}. \quad (9.82)$$

Specifically, Eq. (9.82) predicts, that the mode with number $m = m_0/2$, i.e. the mode at half the center frequency, does not change its frequency

as a function of intracavity pulse energy. Of course, one has to remember, that this model is so far based on self-phase modulation and self-steepening as the cause of a power dependent carrier-envelope offset frequency. There may be other mechanisms that cause a power dependent carrier envelope offset frequency. One such effect is the group delay caused by the laser gain medium another one is the carrier-envelope change due to a change in carrier frequency, which gives most likely a very strong additional dependence on pump power. Nevertheless, the formula 9.82 can be used for the control of the optical frequency comb of a femtosecond laser by controlling the cavity length and the intracavity pulse energy, via the pump power.

9.4 Femtosecond Laser Frequency Combs

Nevertheless, the formula (9.82) can be used for the control of the optical frequency comb of a femtosecond laser by controlling the cavity length and the intracavity pulse energy, via the pump power. According to Fig. 9.2 every line of the optical comb determined by

$$f_m = f_{CE} + m f_R. \tag{9.83}$$

Note, if the femtosecond laser emits a spectrum covering more than one octave, then one can frequency double part of the comb at low frequencies and beat it with the corresponding high frequency part of the comb on a photo detector, see Fig. 9.5 The result is a photodector beat signal that consists of discrete lines at the beat frequencies

$$f_k = k f_R \pm f_{CE} \tag{9.84}$$

This method for determining the carrier-envelope offset frequency is called f-to-2f interferometry.The carrier-envelope offset frequency can be extracted with filters and synchronized to a local oscillator or to a fraction of the repetition rate of the laser, for example $f_R/4$.

Figure 9.6 shows the setup of an octave spanning 200 MHz Ti:sapphire laser where the carrier envelope offset frequency f_{CE} is locked to a local oscillator at 36 MHz using the f-to-2f self-referencing method [6]

The spectral output of this laser is shown in Figure 9.7 The spectral components at 1140 are properly delayed in a chirped mirror delay line against the spectral components at 570 nm. The 1140 nm range is frequency doubled in a 1mm BBO crystal and the frequency doubled light together with

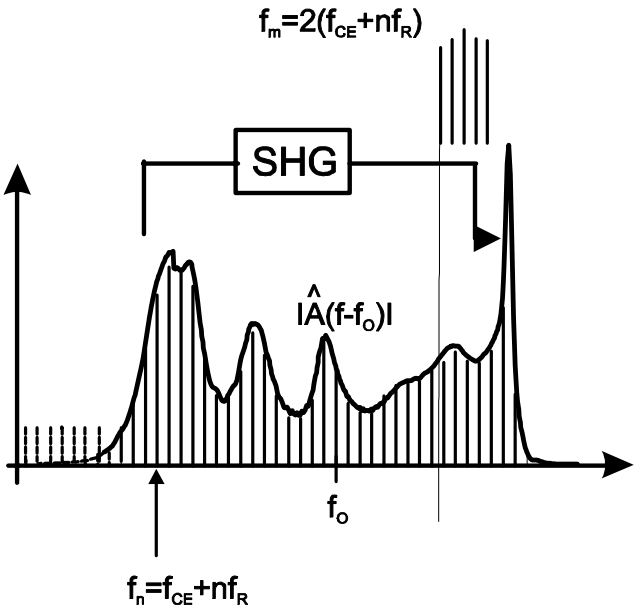

Figure 9.5: f-to-2f interferometry to determine the carrier-envelope offset frequency.

Image removed due to copyright restrictions.

Please see:
Mucke, Oliver, et al. "Self-Referenced 200 MHz Octave-Spanning Ti: Sapphire Laser with 50 Attosecond Carrier-Envelope Phase Jitter." *Optics Express* 13, no. 13 (June 2005): 5163-5169.

Figure 9.6: Carrier-envelope phase stabilized 200 MHz octave-spanning Ti:sapphire laser. The femtosecond laser itself is located inside the grey area. AOM, acousto-optical modulator; S, silver end mirror; OC, output coupling mirror; PBS, polarizing beam splitter cube; PMT, photomultiplier tube; PD, digital phase detector; LF, loop filter; VSA, vector signal analyzer. The carrier-envelope frequency is phase locked to 36 MHz.

Figure 9.7: Output spectrum of the Ti:sapphire laser on a linear (black curve) and on a logarithmic scale (grey curve). The wavelengths 570 and 1140 nm used for self-referencing are indicated by two dashed lines.

the fundamental at 570 nm is projected into the same polarization via a polarizing beam splitter. The signal is then filtered through a 10nm wide filter and detected with a photomultiplier tube (PMT). A typical signal from the PMT is shown in Figure 9.8.Phase locking is achieved by a phase-locked loop (PLL) by feeding the error signal from the digital phase detector to an AOM placed in the pump beam (see Fig. 9.6) which modulates the pump power and thus changes the carrier-envelope frequency via Eq.(9.82). A bandpass filter is used to select the carrier-envelope beat signal at 170 MHz. This signal is amplified, divided by 16 in frequency, and compared with a reference frequency fLO supplied by a signal generator (Agilent 33250A) using a digital phase detector. The carrier-envelope beat signal is divided by 16 to enhance the locking range of the PLL. The phase detector acts as a frequency discriminator when the loop is open, the output is thus the difference frequency between the carrier-envelope frequency and the designated locking frequency. The output signal is amplified in the loop filter, which in our case is a proportional and integral controller, and fed back to the AOM, closing the loop. The output of the phase detector is proportional to the remaining jitter between the carrier-envelope phase evolution and the local oscillator reduced by the division ratio 16. The power spectral density (PSD) of the carrier-envelope phase fluctuations are measured with a vector signal analyzer (VSA) at the output of the phase detector. After proper rescaling by the division factor the phase error PSD is shown in Fig. 9.9. The measure-

Figure 9.8: Radio-frequency power spectrum measured with a 100 kHz resolution bandwidth (RBW). The peak at the carrier-envelope frequency offset frequency exhibits a signal-to-noise ratio of ~35 dB.

ment was taken in steps with an equal amount of points per decade. The PSD of the carrier-envelope phase fluctuations can be integrated to obtain the total phase error. In the range above 1 MHz (see Fig. 9.9), the accuracy of this measurement is limited by the noise floor of the vector signal analyzer. We obtain an integrated carrier-envelope phase jitter of about 0.1 radian over the measured frequency range. The major contribution to the phase noise comes from low frequency fluctuations <10 kHz. If in addition to the carrier-envelope frequency also the repetition rate of the laser is locked to a frequency standard, such as for example a Cesium clock, the femtosecond laser frequency comb in the optical domain is completely determined with microwave precision and can be used for optical frequency measurements [6].

Figure 9.9: Carrier-envelope phase noise power spectral density (left) and integrated phase jitter (right) resulting in only 45 as accumulated carrier-envelope timing jitter.

Bibliography

[1] H.A. Haus and A. Mecozzi: Noise of mode-locked lasers, IEEE J. Quantum Electron. **29**, 983-996 (1993).

[2] S. Namiki and H. A. Haus: "Observation of nearly quantum-limited timing jitter in a P-APM all fiber ring laser", J. of the Opt. Soc. of Am. B., 13, 2817-2823 (1996).

[3] S. Namiki and H. A. Haus: "Noise of the stretched pulse fiber ring laser: Part I–Theory", IEEE J. of Quantum Electronics, 33, 640-659 (1997).

[4] Ch. Xu, S. Namiki, H. A. Haus: "Noise in the Streched Pulse Fiber Laser: Part II – Experiments", IEEE J. of Quantum Electronics, 33, 660-668 (1997).

[5] H.A. Haus and E.P. Ippen: Group velocity of solitons, Opt. Lett. **26**, 1654-1656 (2001)

[6] D. J. Jones, S. A. Diddams, J. K. Ranka, R. S. Windeler, J. L. Hall, and S. T. Cundiff, Science **288**, 635 (2000).